

Efficient Numerical Simulations of the Time Dependence of Electronic Energy Transfer in Polymers. 2. Short-Range Transfer and Förster Trapping

Jeffrey D. Byers, W. Samuel Parsons, Richard A. Friesner, and S. E. Webber*

Department of Chemistry and Center for Polymer Research, University of Texas at Austin, Austin, Texas 78712

Received December 18, 1989; Revised Manuscript Received April 21, 1990

ABSTRACT: Calculations have been carried out of the time dependence of a donor excited state in the presence of down-chain electronic energy transfer between polymer segments with simultaneous trapping by a Förster dipole-dipole mechanism. The donor excited-state survival probability (fluorescence decay) has been analyzed in terms of an effective dimensionality with the objective of testing explicit conformational models for polymers. It has been found that long-range trapping obscures the fractal dimensionality characteristics of these systems. A discussion is presented concerning the sensitivity of methods for extracting conformational properties of polymers from fluorescence decay measures.

Introduction

In recent years there has been considerable effort in the field of polymer photophysics,¹⁻³ both from the point of view of exploiting the special photophysical properties exhibited by polymers and with the objective of using these photoprocesses to elucidate the nature of the polymer conformation and morphology. The present paper has the latter objective, applied to polymers that have a high concentration of chromophores, such that extensive nearest-neighbor electronic energy transfer (EET) can occur. The present calculations extend our earlier work in which only nearest-neighbor transfer and trapping were considered.⁴ Our calculations are based on a simple self-avoiding lattice model with an intersegmental contact energy (denoted by $\phi = -\epsilon/kT$, where ϵ is the contact energy), and we use the Lanczos algorithm to compute the decay curve for each member of the polymer ensemble. Our objective in our initial effort was to understand how intersegmental contacts affected the rate of energy trapping. In general, the rate of energy trapping was found to increase steadily as the polymer coil became more compact, as one would expect intuitively. However, the detailed behavior of the fluorescence decay is quite complex. Very recently van Rensburg et al. have also considered computer simulations of EET on a self-avoiding polymer coil.⁵ While they did not consider the effect of the solvent-polymer interaction, certain scaling ideas applied to polymer EET were tested.

In the present calculations we permit the trapping of the migrating excited state to occur via the Förster dipole-dipole mechanism.⁶ Since there has been significant theoretical work on single-step energy transfer to traps,⁷⁻⁹ we compare this to the case in which there is simultaneous down-chain, nearest-neighbor EET and Förster trapping.¹⁰ Our goal in this comparison is to discover what, if any, conformational information is available in each case.

We also discuss the inversion of experimental decay data to obtain physical parameters of the polymer (e.g., density of traps or ϕ). One major difficulty that must be faced is that the predicted decay curves are very nonexponential and it is not obvious which of the many ways they could be analyzed is most revealing of the underlying polymer structure. The ability to fit experimental data does not uniquely establish the validity of a particular conformational model, such that it is important to analyze how to

treat experimental data in a consistent fashion. Our confidence in using time-dependent fluorescence data to understand polymer conformations will have to be established as the result of experience in using model simulations to fit experimental data.

It should be mentioned that the present efforts can also be applied to the design of photon-harvesting polymers. For example, it is not a priori obvious that the relative photon collection efficiency is increased by increasing the trapping radius if, for some structural reason, this is accompanied by an expansion of the polymer coil, thus diminishing intracoil contacts. When simulations such as those presented herein are carried out, these issues can be explored before undertaking the preparation of a particular polymer.

Summary of the Method

The time-dependent probability of an excitation residing on a particular chromophore can be described by a Pauli master equation

$$dp/dt = \mathbf{W}p \quad (1)$$

where $p_i(t)$ is the probability that the i th chromophore is excited at time t . If all the chromophores are equally likely to have been excited (i.e., $p_i(0) = 1/N$ where N is the number of chromophores), then the total survival probability can be written as

$$S(t) = \sum_{i=1}^N p_i(t) = (1/N) \sum_{i=1}^N R_{ff}^{(i)} \exp(\lambda_i t) \quad (2)$$

where $R_{ff}^{(i)}$ is the residue of the eigenvalue λ_i of \mathbf{W} .^{11,12} The matrix \mathbf{W} is directly related to the conformation of the polymer, since the transfer rate from the i th to the j th chromophore depends on their separation. For the calculations presented herein the elements of \mathbf{W} are given by

$$\begin{aligned} W_{ij} &= 1/\tau \quad \text{if } i \text{ and } j \text{ are nearest neighbors on} \\ &\quad \text{the lattice} \\ &= (R_0/R_{ij})^6(1/\tau) \quad \text{if } i \text{ or } j \text{ is a trapping species} \\ W_{ii} &= -[n_i + \sum_t (R_0/R_{it})^6](1/\tau) \end{aligned} \quad (3)$$

where n_i is the number of nearest neighbors of the i th site (excluding any that are occupied by traps) and the sum over t represents the number of traps on the polymer chain.

The fundamental energy transfer time between neighboring sites is given by τ . While this is obviously a gross simplification (see Discussion of the Polymer Model), it is common to much work in this general area. The sites that are occupied by traps are not included in \mathbf{W} because it is assumed that no EET occurs out of a trap. Obviously \mathbf{W} varies for each member of the polymer ensemble, such that the observed fluorescence decay is an ensemble average:

$$\langle S(t) \rangle = \sum S_m(t) \pi_m^{-1} e^{-U_m/kT} / \sum \pi_m^{-1} e^{-U_m/kT} \quad (4)$$

In eq 4 U_m is the energy of the m th member of the ensemble, given by $-C_m\epsilon$, where C_m is the number of nonbonding contacts between segments in the m th member of the ensemble. Thus a negative value of ϵ/kT ($=-\phi$) implies that segmental contacts are disfavored (a good solvent) and the coil expands. A positive value of ϕ has the opposite effect. The quantity π_m in eq 4 represents importance sampling for the m th ensemble to take into account the different probabilities of the individual steps used to generate the polymer on the lattice. In all cases only single occupation of the lattice site is possible, such that the polymer is self-avoiding.¹³

The key to our method is the use of the Lanczos algorithm to find the eigenvalues and residues of the large number of \mathbf{W} matrices generated in the ensemble. This algorithm is effective if the \mathbf{W} matrix is sparse, which will be the case so long as the number of intracoil nonbonding contacts is a small fraction of the total number of chromophores. While the results presented herein are for EET on a polymer coil, the methods are perfectly general and have been applied to a number of problems involving EET on lattices. The primary limitation in our approach is that the \mathbf{W} matrix is time-independent, which is appropriate for either an immobilized polymer or a very short lifetime excited state.

Discussion of the Polymer Model

The model we explore in this paper is a highly simplified representation of a real polymer that ignores numerous effects of possible significance (e.g., chromophore orientation). While this model is expected to provide insight as to the thermodynamic implications of a self-avoiding walk, ignoring the molecular details of the repeating units makes it difficult to interpret the τ values in eq 3 or what is meant by a nonbonding contact with respect to the photophysical processes. For a real polymer whose motions are frozen one expects a wide range of interchromophore separation and/or orientations, with a concomitant variation in the energy-transfer rate. It is our intention to explore these effects in future papers in this series, but it is reasonable to consider our motivation in studying the present model and to discuss when it might be expected to have some degree of physical reality.

First, the objective of the present work is to systematically explore the effect of varying fundamental physical features of the model (e.g., trapping radius) with regard to analysis fluorescence decay data. As argued below, we believe that such fundamental studies are a necessary predecessor to the development of reliable analysis procedures for experimental data.

Second, we wish to understand if there is any real hope of extracting conformational information from the very complex fluorescence decay curves that result when there is simultaneous EET and trapping. If even for such a simplified model as presented here there were a large number of decay curves that were sensibly identical, then further detailed modeling would not seem profitable. It

is because of our interest in interpreting experimental decay curves that we spend considerable effort in this paper discussing what we believe are useful methods of characterization and analysis. As will be discussed later, it does seem as though with proper treatment of fluorescence decay curves a unique fit of a decay curve to the present model can be achieved.

Since we ignore time-dependent changes of the polymer coil, the coil must be regarded as frozen on the time scale of the excited state. On the other hand the assumption of a constant transfer rate implies that either all chromophores are identically oriented and separated or, more realistically, there are local motions that average out individual differences on the time scale of the excited state. Thus this model might be valid for a polymer in a viscous liquid. Another case in which the present model might be valid is if groups of chromophores are treated jointly, as a kind of "photophysical blob". In this case the individual variations in molecular orientations and separation would tend to be averaged out and τ would represent the average transfer between "blobs". This would seem to be especially appropriate if the Förster R_0 for self-transfer were larger than the average chromophore separation.

Excimer traps represent an example of a short-range trapping species, whose concentration depends not only on the tacticity of the polymer but also on the polymer conformation, as has been studied extensively by Frank and co-workers.¹⁴ Thus in this case we expect a relation between the trap density (p) and the thermodynamic parameter ϕ . Later in this paper we discuss the possibility for obtaining these two parameters independently from the model presented herein. In certain cases the excimer can dissociate to reform the monomeric excited state, which greatly complicates the kinetics of the monomer excited state, as discussed by Sienicki and Mattice,¹⁵ Sienicki and Winnik,¹⁶ and Martinho and Winnik.¹⁷ However, these workers have shown that excimer dissociation can be handled by an additional convolution integral involving the decay of the donor (monomer) excited state, such as we calculate in this paper.

Direct Energy Transfer

Direct energy transfer (DET) involves a single step from a donor to an array of independent acceptors with a rate constant that depends on R_0/R_{ij} .⁶ Because this process depends on a pairwise distribution of separations, it has been subjected to considerable theoretical analysis, including the original work by Förster. Klafter and Blumen¹⁸ have considered this problem for general geometries of infinite size and derive the following:¹⁹

$$\ln \Phi(t) = -p \int d\mathbf{r} \rho_0(r) \{1 - \exp(w(\mathbf{r})t)\} \quad (5a)$$

$$= -A_0 \Gamma(1 - d/6) (t/\tau_D)^{d/6} \quad (5b)$$

In eq 5 $\Phi(t)$ is the survival probability of the donor excitation and is equivalent to $\langle S(t) \rangle$ in eq 4. The quantity p is the fraction of lattice sites occupied by traps, and it is assumed that $w(r) \propto 1/r^6$ (the Förster mechanism). The intrinsic decay of the donor has been disregarded (this amounts to multiplying an experimental curve by e^{+t/τ_D}). In eq 5 A_0 is expected to be proportional to the density of traps and the overall geometry of the system, τ_D is the intrinsic lifetime of the donor excited state, $\Gamma(x)$ is the gamma Euler function, and d is the fractal dimensionality of the system. This latter quantity is related to the density

of lattice points according to

$$\rho(r) \propto r^{d-d} \quad (6)$$

in which d is the Euclidean dimension and r is the distance from the origin of the coordinate system. For a classical system $d = d$ and one obtains an exponential decay for $\Phi(t)$, which depends on $t^{1/2}$, $t^{1/3}$, or $t^{1/6}$ for 3-, 2-, and 1-dimensions, respectively.

It has been argued previously by one of us²⁰ that the radius of gyration (R_g) of a polymer may be used to determine d in eq 6. R_g may be related to the degree of polymerization (N) according to

$$R_g \propto N^a \quad (7)$$

from which it follows

$$\rho(R_g) \propto N/R_g^3 \propto R_g^{1/a-3} \quad (8)$$

such that

$$d = 1/a \quad (9)$$

The Mark-Houwink parameter (β) is related to the inverse of the coil density

$$\rho(R_g)^{-1} \propto N^\beta \quad (10)$$

leading to the relation

$$d = 3/(1 + \beta) \quad (11)$$

Thus for an infinite coil that obeys eqs 7 and 8 we would expect a simple variation in d obtained from intracoil DET as a function of coil expansion.

The calculation of $\langle S(t) \rangle$ for this model is very simple using our methods, and some typical decay curves are presented in Figure 1. These curves are very different from those in which down-chain EET occurs, as one might expect (cf. Figure 1 and Figure 4). In particular, for DET at long times the rate of decay becomes much slower, due to contributions from the members of the donor-trap ensemble that are located far from each other.

These decay curves can be analyzed in terms of an "apparent dimensionality",⁷ which is defined by

$$\alpha(t) = -d\{\ln(\ln \langle S(t) \rangle)\}/d\{\ln(t)\} \quad (12)$$

Note that $\alpha(t)$ is equivalent to $d/6$ in eq 5. We have found the $\alpha(t)$ function to be revealing in our earlier analysis of down-chain EET.⁴ The behavior of $\alpha(t)$ is distinctly different for DET and down-chain EET. Examples of the former are given in Figure 2 for the same decay curves as Figure 1. While these plots demonstrate a strong dependence on R_0 , there are certain common features: (1) Initially $\alpha(t)$ decreases and approaches an asymptotic limit at relatively early times (compare this to plots discussed below). The early time values are on the order of 0.27–0.35, while at long time, $\alpha(t)$ approaches 0.23–0.27. (2) In several cases $\alpha(t)$ does not display a particularly strong dependence on ϕ , but there is a complicated interplay of chain length and R_0 . We have not found a simple dependence on R_0/R_g . We note that from the simple considerations embodied in eqs 7–10 we would expect $d/6$ to be equal to $1/3$ for a Θ solvent, and for $\beta = 1$ (an expanded coil) $d/6 \approx 1/4$. While the observed values of $\alpha(t)$ fall roughly in this range, they do not respond systematically to ϕ (which should affect β most strongly). This suggests that an analysis like that of Levitz et al.,⁷ which does not take into account finite size effects, is oversimplified for polymer systems of the type discussed herein.

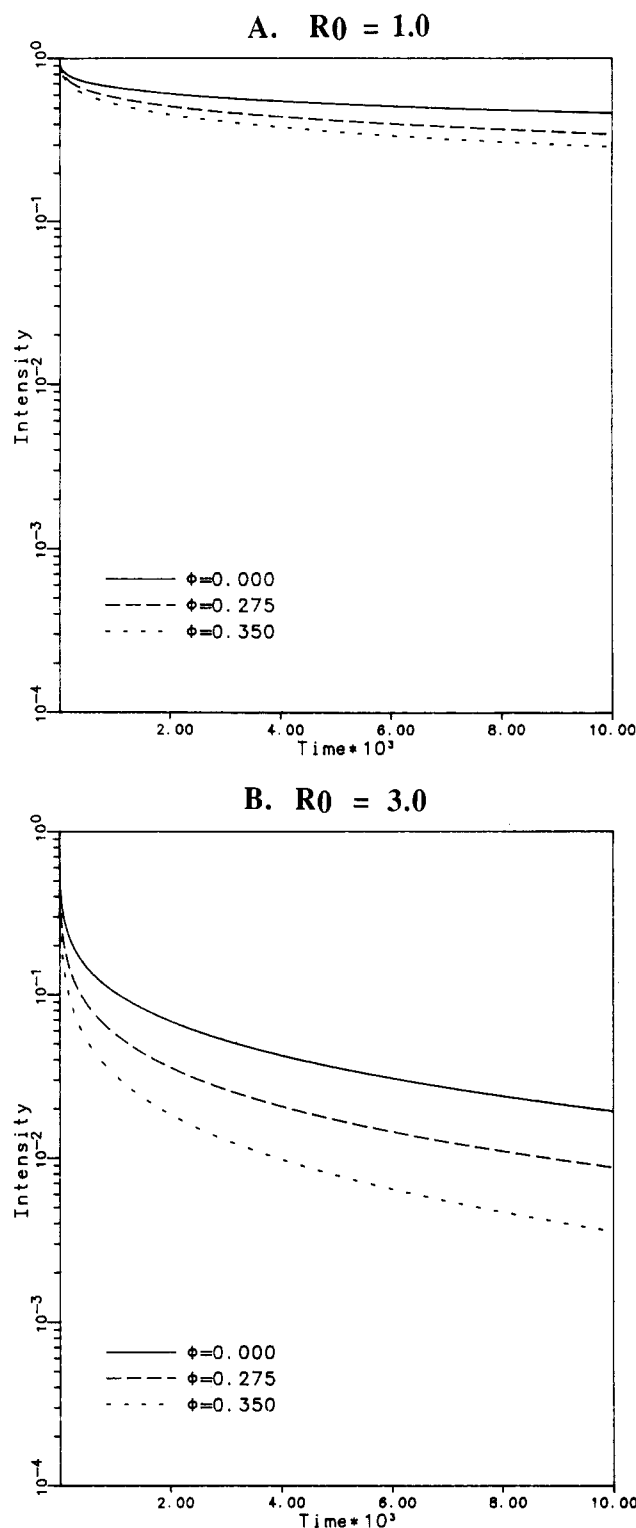


Figure 1. Decay curves for DET for the ϕ value indicated. For all cases the trap density (ρ) is 0.02 and $N = 100$: (A) $R_0 = 1.0$, (B) $R_0 = 3.0$.

One may also fit the decay functions to a "stretched exponential" (which is equivalent to eq 5 with $\alpha = d/6$)

$$\langle S(t) \rangle = \exp(-At^\alpha) \quad (13)$$

in which A and α are both independent of time. A reasonably good fit can be obtained in all cases, but the values of α are essentially independent of ϕ although the values of A increase with both ϕ and N (Table I). While a stretched exponential seems to be a natural fitting function for decays of this type, the absence of a systematic variation of both α and A with ϕ implies that this is not

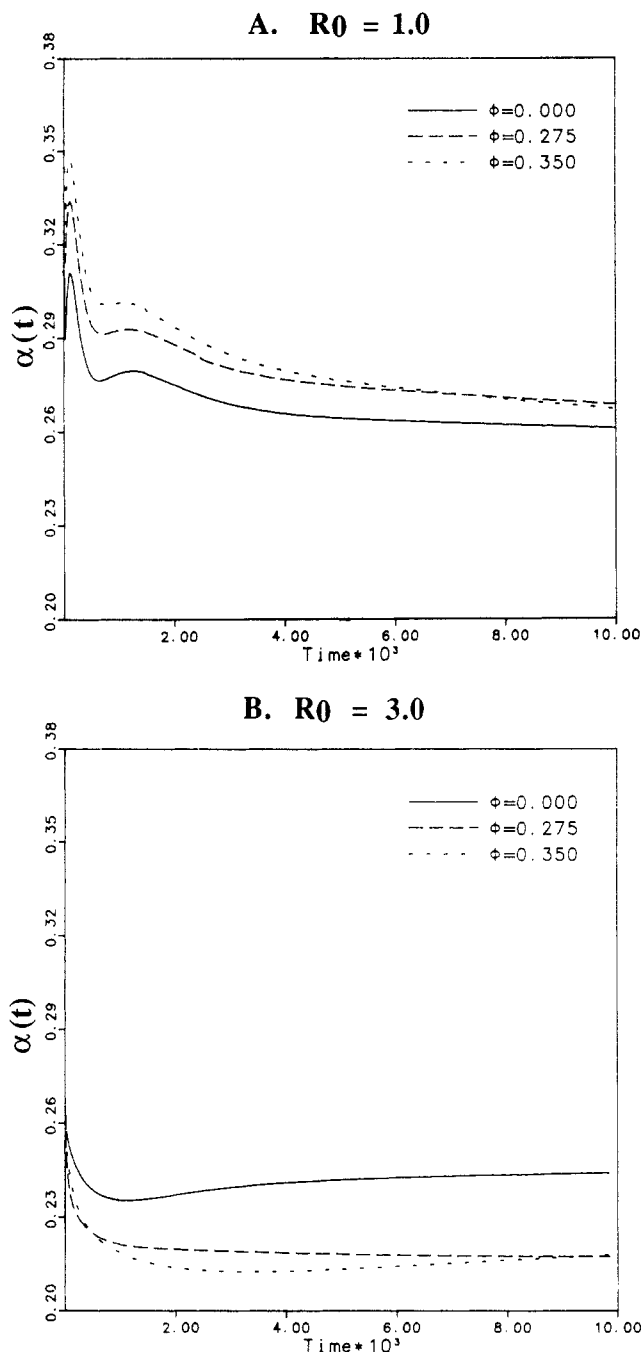


Figure 2. $\alpha(t)$ curves (defined by eq (12) for the same decay curves as Figure 1: (A) $R_0 = 1.0$, (B) $R_0 = 3.0$).

likely to be a satisfactory approach to obtain polymer conformational parameters.

The failure of the stretched exponential to satisfactorily describe the single step decay of our polymer systems can be understood because eq 6 is not valid for finite systems at large values of r . For finite systems the following conditions must hold

$$\int_0^\infty 4\pi r^2 \rho(r) dr = N$$

$$\lim_{r \gg Na} \rho(r) = 0 \quad (14)$$

where N is the number of segments and a is the segment length. In plots of the pairwise radial distribution function $g(r) = 4\pi r^2 \rho(r)$ (see Figure 3) these finite size effects are easily seen. At large r , $g(r)$ falls rapidly to zero, unlike an infinite fractal system. At small r the behavior is close to that described by eq 6; i.e., when the polymer is

Table I
Fitting Parameters Obtained from Equation 13 for DET^a

size	R_0	ϕ	d	α^b	A
50	3.0	0.0	1.58	0.263	0.41
		0.275	1.51	0.252	0.55
		0.35	1.52	0.253	0.61
	1.5	0.0	1.65	0.275	0.12
		0.275	1.63	0.272	0.16
		0.35	1.64	0.273	0.17
	1.0	0.0	1.71	0.285	0.057
		0.275	1.76	0.293	0.070
		0.35	1.77	0.295	0.076
100	3.0	0.0	1.35	0.225	0.47
		0.275	1.34	0.223	0.63
		0.35	1.30	0.217	0.77
	1.5	0.0	1.56	0.260	0.13
		0.275	1.55	0.259	0.19
		0.35	1.55	0.258	0.22
	1.0	0.0	1.68	0.280	0.059
		0.275	1.68	0.280	0.080
		0.35	1.72	0.287	0.086
200	3.0	0.0	1.30	0.217	0.51
		0.275	1.21	0.202	0.76
		0.35	1.14	0.190	0.99
	1.5	0.0	1.59	0.265	0.13
		0.275	1.51	0.252	0.20
		0.35	1.47	0.245	0.26
	1.0	0.0	1.66	0.277	0.062
		0.275	1.70	0.283	0.083
		0.35	1.73	0.288	0.098

^a All for a trap density (p) equal to 0.02. ^b $\alpha = d/6$.

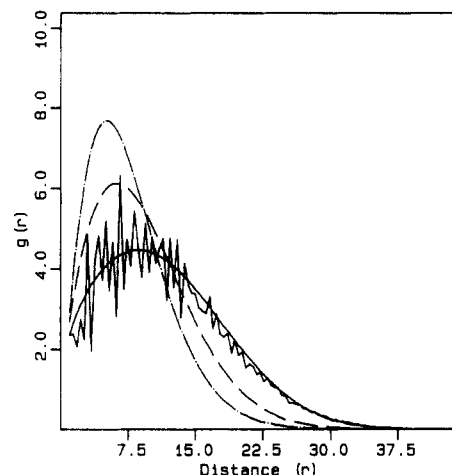


Figure 3. Plot of pairwise radial distribution function $g(r)$ for polymer simulation and fit using eq 15 (smooth solid line) for $\phi = 0$ (bottom curve). Other smooth broken curves are fits to $g(r)$ for $\phi = 0.275$ (middle) and 0.350 (top).

collapsed, the fractal dimension of the polymer increases and $g(r)$ increases at a faster rate. So the higher dimension systems have a higher value of $g(r)$ than the lower dimension systems at small values of r . However, at longer distances the reverse is true and the lower dimension systems have a larger value of $g(r)$. This is a direct result of the normalization of $g(r)$, which is independent of coil density.

This phenomenon is very important to the long-time behavior of $\langle S(t) \rangle$ and $\alpha(t)$. The early time decay should follow the result given in eq 5, since the large distance interactions are negligible in this time period. However, at longer times these long-range transfers will dominate and hence the behavior of $g(r)$ at large r will become extremely important. Qualitatively the falloff of $g(r)$ resembles a Gaussian tail, similar to the end-to-end distance distribution functions for random-walk polymers. It was possible to fit the total radial distribution function

Table II
Fitting Parameters Obtained from Equation 15

size	ϕ	$\langle C_i \rangle$	δ	a	ν
50	0.0	2.34	1.22	1.97×10^{-2}	2.02
	0.275	2.56	1.36	3.54×10^{-2}	1.94
	0.35	2.67	1.60	1.11×10^{-1}	1.58
100	0.0	2.34	1.37	1.39×10^{-2}	1.87
	0.275	2.63	1.47	1.84×10^{-2}	1.91
	0.35	2.79	1.65	4.71×10^{-2}	1.68
200	0.0	2.35	1.36	8.71×10^{-4}	2.46
	0.275	2.69	1.60	1.48×10^{-2}	1.78
	0.35	2.92	1.90	6.27×10^{-2}	1.46

to the form ($r \geq 1$)

$$g(r) = Ar^{\delta-1} \exp(-a(r-1)^\nu) \quad (15)$$

with δ , a , and ν serving as the adjustable fitting parameters. This functional form is similar to that used to model end-to-end distribution functions for random-walk polymers.²¹ The value for A was fixed at the average number of segmental contacts ($\langle C_i \rangle$) in order to reduce the number of adjustable parameters. As can be seen from Figure 3, this function fits the computer-generated $g(r)$ function very well. Table II contains the fitting parameters obtained. At small r , such that the exponential term can be ignored, a comparison of eqs 6 and 15 suggests the identification of δ with d . We note that δ does increase with ϕ (Table II), but it is also a function of chain length.

On the other hand, there is a very systematic variation in the decay curves $\langle S(t) \rangle$ with ϕ (see Figure 1) and it seems likely that a direct comparison of simulated and experimental decay curves may be the most accurate method for extracting conformational parameters from DET experiments. In fact, this is the method that has been employed successfully by Fayer and co-workers in polymer blends.⁸ We will discuss the general problem of fitting conformational models to observed decays in a later section.

Down-Chain EET with a Förster Trap

For these calculations there is simultaneous down-chain EET between all nearest neighbors on the lattice (bonded or nonbonded) and Förster transfer to the trap species (i.e., the full matrix from eq 3). As would be expected, the survival probability decays much more rapidly than the corresponding DET case (cf. Figure 4 and Figure 1). The results for $R_0 = 1$ are very similar to our previous calculations in which trapping occurred only at nearest neighbors,⁴ as would be expected. The $\alpha(t)$ curves (Figure 5) have a character strikingly different from those for DET. In particular, the curves in Figure 5 often have minima at early times and either increase continuously or appear to reach an asymptotic limit.²² Additionally, the values of $\alpha(t)$ tend to be larger in the presence of down-chain EET than in its absence (cf. Figures 2 and 5). However, the interplay of the parameters of chain length (N), density of traps (p), and thermodynamic interaction (ϕ) is very complex, such that it seems likely that any analysis of experimental data will require an empirical approach. We describe two such efforts in the next section.

Since DET has been used by several workers to assess the dimensionality of a physical system, it is appropriate to compare the sensitivity of DET and EET to polymer conformation, as influenced by ϕ . If one compares the curves for DET and EET in Figures 1 and 4, respectively, it is clear that $\langle S(t) \rangle$ is equally sensitive to the ϕ values for $R_0 = 3$ for both cases, but the EET curves are much more dependent on ϕ for $R_0 = 1$. This is as one would expect because in the absence of down-chain EET a trapping species with a small R_0 is sensitive to a relatively

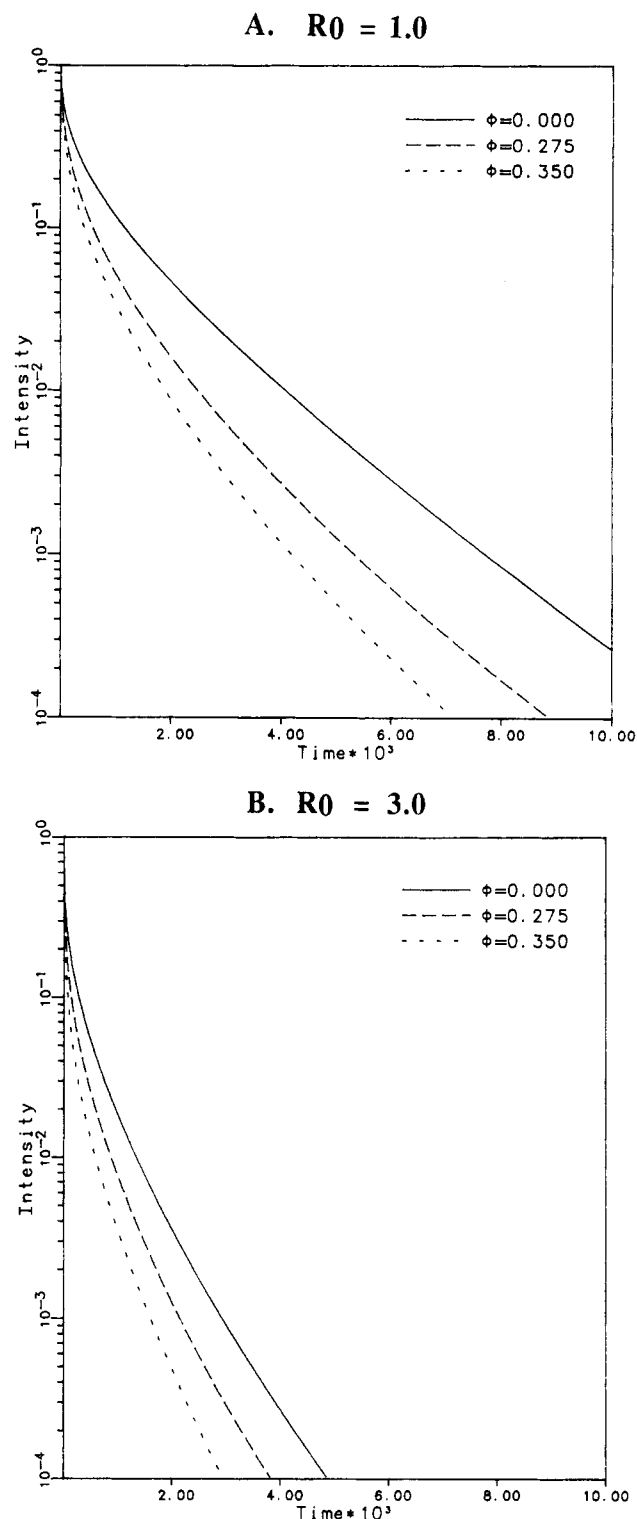


Figure 4. Decay curves for simultaneous down-chain EET and Förster trapping (cf. Figure 1): (A) $R_0 = 1.0$, (B) $R_0 = 3.0$.

small fraction of the segmental distribution function ($p(r)$ in eq 5a or eq 14). An advantage of the present computational scheme is that the effect of polymer conformational changes on a relatively complex set of EET processes can be explicitly evaluated.

Inversion of Experimental Decay Data To Obtain Model Parameters

Our earliest calculations and those presented above demonstrate that fluorescence decay curves in the presence of DET or EET are sensitive to the coil density, the mole fraction of traps, and the degree of polymerization. It is

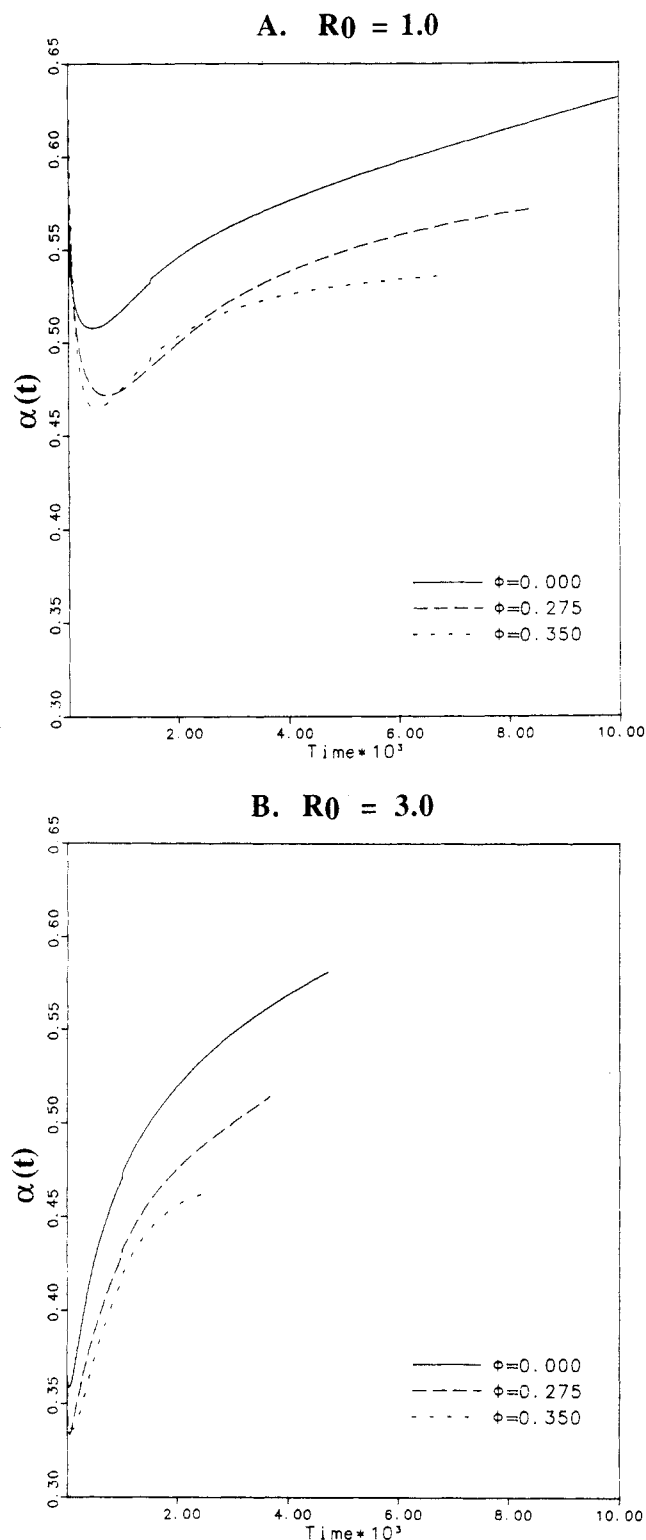


Figure 5. $\alpha(t)$ curves for the decay curves of Figure 4: (A) $R_0 = 1.0$, (B) $R_0 = 3.0$.

also obvious that more complex polymer models could be treated in a similar fashion. The question we now address is the "inversion" of this problem. That is, if we have a model we believe is appropriate to a given polymer system and we have the fluorescence decay for that system, how can we obtain the conformational parameters? While it seems likely that no polymer model can uniquely fit fluorescence decay data, even within the context of a given model, it is not necessarily the case that a unique set of parameters will emerge.

We approach this problem in two ways. In the first approach we find a polynomial representation of the

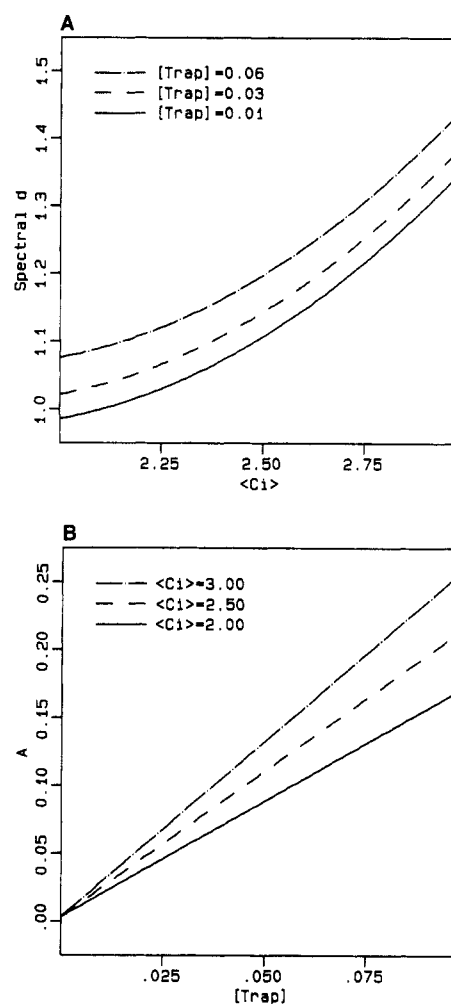


Figure 6. (A) Plot of d_s as a function of $\langle C_i \rangle$ for indicated trap densities (p). (B) plot of A as a function of p for different $\langle C_i \rangle$ values.

variation of some parameter of the fluorescence decay fitting function in terms of the polymer model. In the second approach we use a "library" of decay curves and find the best match between an experimental decay curve and the library set. For the EET case we find that matching $\alpha(t)$ curves (eq 12) is more successful than using the decay curves themselves.

(a) Polynomial Method for EET with $R_0 = 1$. In our earlier paper we noted that the behavior of the $\alpha(t)$ curve varied in a regular way as a function of ϕ^4 . This regularity was expressed by the behavior of the initial value of $\alpha(t)$ ($\alpha(0) = \alpha_i$), the value of $\alpha(t)$ at its minimum ($\alpha(t_{\min}) = \alpha_{\min}$), and the time required to reach this minimum (t_{\min}). We also examined fitting the decay curve to an exponential polynomial of the form

$$\langle S(t) \rangle = \exp(-At^{d_s/2} + Bt^{d_s} - Ct^{3d_s/2}) \quad (16)$$

over the time span from zero to t_{\min} . In this expression d_s represents the effective spectral dimension and the constants A – C can be related to the different cumulants of the number of unique steps taken on a lattice. According to this model, A should be proportional to $\ln(1-p) \approx p$. In practice we treat all these as fitting parameters.

Following this prescription, we find that all these parameters vary systematically with N , p , and ϕ . We also find that this variation is systematic in N , p , and $\langle C_i \rangle$ (the average number of segmental contacts). Because $\langle C_i \rangle$ has a direct physical significance, we prefer to use it in the following. In Figure 6 we plot the variation of d_s with $\langle C_i \rangle$

for several different trap densities and A as a function of trap density for several different $\langle C_i \rangle$ values. The former increases monotonously as the coil is contracted and $\langle C_i \rangle$ increases, as one would expect from the physical interpretation of the spectral dimension (recall that $d_s = 1$ and 2 for an infinite 1D and 3D lattice, respectively). A depends almost linearly on p , and as the coil becomes more compact the apparent efficiency of trapping increases (note the increased slope of the A vs p curve as a function of $\langle C_i \rangle$). The variations with N are equally systematic but are not shown for clarity.

These variations can be fit to an empirical polynomial, and then experimental values of A and d_s can be used to solve the resulting algebraic equations for the parameters of the model. Questions remain of whether the solution is multiple valued and whether it is sufficiently well-behaved that reasonably accurate values can be obtained. Obviously there are many different combinations of N , p , and $\langle C_i \rangle$ that can be used for the empirical polynomial. We tried a number of possibilities and selected the particular form that provided the best fit while maintaining the maximum degree of linear independence. The best choice we found was

$$A = 0.00354 + (0.877\langle C_i \rangle - 0.0498)p + 5.09(p/N) \quad (17)$$

$$d_s = 1.79 + 1.81p - 0.934\langle C_i \rangle + 4.12(\langle C_i \rangle/N) \quad (18)$$

One may take an experimental decay curve and fit it according to eq 16. The experimental values of A and d_s are then inserted into eqs 17 and 18 and the plots of $\langle C_i \rangle$ vs p generated (for the moment we assume that N is known). If these curves cross only once for physically realistic values of these parameters, then we have a unique solution for p and $\langle C_i \rangle$. If the two curves cross nearly perpendicularly, then the solution is well-conditioned and can be expected to yield reasonably accurate values.

Two examples of this approach are given in Figure 7. For this calculation a decay curve from our ensemble was selected to be fit (hence, the values of N , p , and ϕ are known). The crossing point of the p vs $\langle C_i \rangle$ curves from eqs 17 and 18, respectively, is reasonably close to the known value of p and $\langle C_i \rangle$ (see Figure 7). For most cases we find that this method yields very satisfactory results. This approach is convenient because empirical expressions like eqs 17 and 18 can be generated for a given model and then used by the experimentalist without having access to the simulation program. However, for this method to work there must be a systematic variation in the fitting parameters with the model parameters. This does not seem to be the case for $R_0 > 1$ or DET using the fitting procedure described above. In particular, d_s is almost independent of ϕ for a given polymer length and trap density. Of course there may be other approaches to analyzing these decay curves that will permit an empirical polynomial relationship to be derived that can be used as described above.

All the simulations are carried out in arbitrary time steps that correspond to the time required for a single EET step between neighboring groups. Relating this to a physical time can be accomplished by scaling the time axis. This will be discussed explicitly in the next section.

(b) Library Method for EET. This method is conceptually straightforward in that it is a brute force comparison of a library of computed decay functions or $\alpha(t)$ plots with an experimental curve. The members of the library are sought that minimize differences in the least-squares sense (the quantity χ^2 in Table IV) and also provide random residuals. Experimental decay curves are obtained in real time while the computed curves are in units of the fundamental transfer time between neighboring chro-

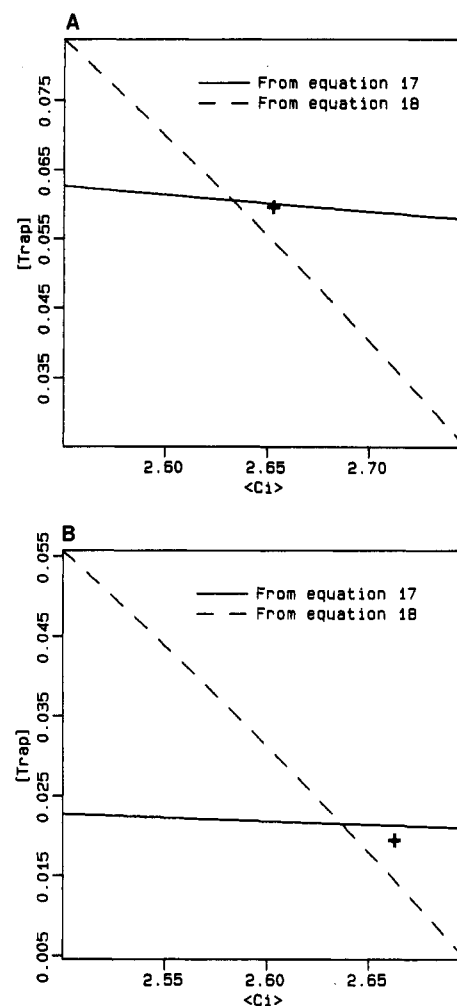


Figure 7. Example of numerical solutions to yield values of ϕ and p . Solid line from eq 17, dashed line from eq 18 for $N = 50$ (A) and 100 (B), respectively. Known values indicated by +.

mophores (τ in eq 3). Consequently, it is also necessary to scale the time axis to provide the best match between the curves. This can be accomplished by either matching the $\langle S(t) \rangle$ curves at some arbitrary amplitude or, as we prefer, matching the time at which the minima in the $\alpha(t)$ curves occur:

$$(t_{\min})_{\text{exp}} = (t_{\min})_{\text{calc}}\tau \quad (19)$$

From this one-point comparison τ is obtained, which is a quantity of direct physical interest from the point of view of EET phenomena.

One consideration in applying this method is the necessity of obtaining a smooth $\langle S(t) \rangle$ curve (or a smooth least-squares fit) for the calculation of $\alpha(t)$. This prevents multiple minima or noisy $\alpha(t)$ curves, which otherwise may be obtained from the calculation. The traditional functional form for fitting decay curves, a sum of exponentials, was tested to find the requirements for an accurate representation. We find that the fit improves with the number of exponentials, as expected, but that at least three or four exponentials are required before the $\alpha(t)$ curve "converges" (see Table III and Figure 8). The experimental data used in this fit is for a random copolymer of methacrylic acid and vinylphenanthrene (42 mol %) with 1.7 mol % of anthracene covalently attached as a trap.²³ When the intrinsic chromophore lifetime was removed (35.1 ns), the calculation required a smaller number of exponential terms to converge but the χ^2 values were larger (see Table III).²⁴ It is important to point out that the quantity $\langle S(t) \rangle$

Table III
Multiexponential Fits to Phenanthrene Decay^a

	no. of exp.	a_1/τ_1	a_2/τ_2	a_3/τ_3	a_4/τ_4	a_5/τ_5	$\chi^2 \times 10^4$	$\langle \tau \rangle^b$
35.1-ns lifetime removed ^c	2	0.87/1.76	0.14/26.6				6.03	19.4
	3	0.71/0.76	0.21/5.47	0.08/31.3			1.000	20.3
	4	0.51/0.50	0.30/1.95	0.12/8.11	0.07/32.8		0.774	20.5
	5	0.51/.50	0.29/1.85	0.06/5.75	0.08/9.31	0.07/32.9	0.770	20.5
	2	0.88/2.50	0.12/222				18.8	205
	3	0.73/0.83	0.20/7.34	0.07/368			10.1	341
	4	0.50/0.49	0.31/1.90	0.13/9.63	0.07/419		9.86	392

^a Dark counts were removed before fitting; $\lambda_{\text{exc}} \approx 285$ nm, $\lambda_{\text{obs}} \approx 360$ nm (phenanthrene fluorescence) for random copolymer of methacrylic acid (58 mol %) and 9-vinylphenanthrene with 1.7 mol % of anthracenemethanol esterified to the acid groups (see ref 16). ^b $\langle \tau \rangle = \sum a_i \tau_i^2 / \sum a_i \tau_i$, the average lifetime. ^c The decay curve is multiplied by e^{+t/τ_D} where τ_D is the intrinsic lifetime of the donor fluorophore.

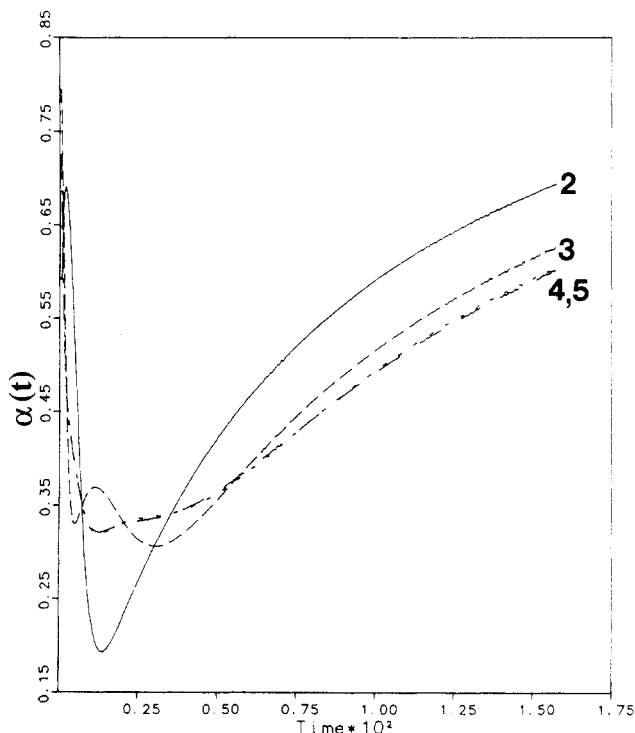


Figure 8. Comparison of $\alpha(t)$ curves for different numbers of exponential functions used in a fit of experimental data.

in eq 12 and elsewhere represents the fluorophore decay from the EET mechanism alone, with the intrinsic lifetime of the fluorophore removed (see the discussion preceding eq 6). We have found that the shape of the $\alpha(t)$ curve is not drastically altered when an experimental curve is multiplied by e^{+t/τ_D} , although the value of α_{min} does change. This suggests that the $\alpha(t)$ curve will not be overly sensitive to the choice of τ_D , which is not always known precisely.²⁵

There are certain disadvantages to a library lookup scheme, such as the possibility of a nonunique set of parameters (see later discussion) and the quality of match obtained is limited by the extent of the library. This last limitation is removed by supplementing the library with the model program to generate decay curves in the "neighborhood" of the best fit. In this manner a sparse library gives a rough estimate of the parameters, and the program iteration provides the refinement. It should be pointed out that it is important to check the statistical variation of the $\alpha(t)$ curves for the ensemble by replica runs with identical physical parameters. The convergence of the $\alpha(t)$ curves for a particular choice of N , p , and ϕ must obviously be complete or the variation due to poor polymer generation statistics can overwhelm the variation from polymer properties.

If some parameters for a given polymer system are known, it is a simple matter to restrict the search, virtually

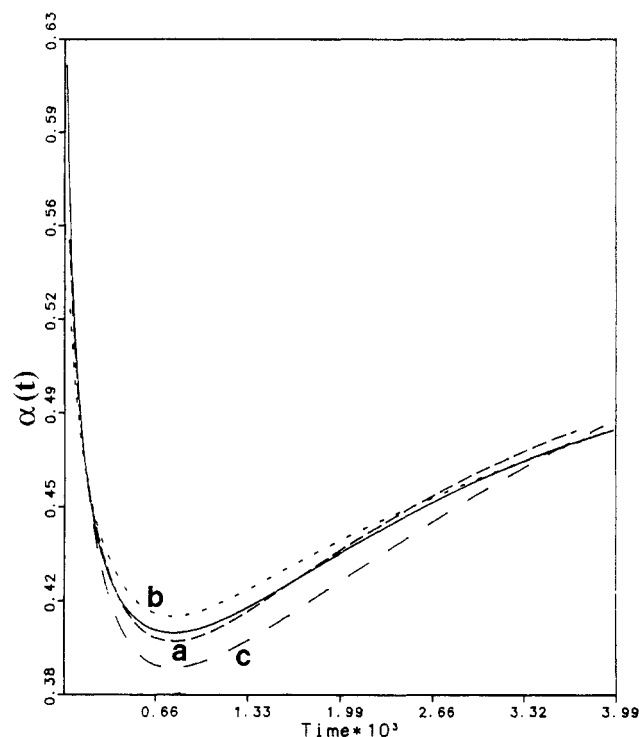


Figure 9. Comparison of an unknown curve (solid line) with three best fits from a library (see Table IV for identification of curves a-c). Note that the time scale is chosen for each curve that provides the best match of α_{min} .

Table IV
Comparison of an Unknown $\alpha(t)$ Curve with Best Fits from a Library Method

curve	length	no. of traps	ϕ	χ^2^b
unknown	75 ^a	4	0.275	
a	100	4	0.275	2.1×10^{-5}
b	100	6	0.0	8.4×10^{-5}
c	50	4	0.0	2.0×10^{-4}

^a Constructed by averaging decay curves for polymers of length 50 and 100 with $\phi = 0.275$ and 4 traps/polymer. ^b Given by $\chi^2 = (n_t - 1)^{-1} \sum (\alpha_i^{\text{unk}} - \alpha_i^{\text{fit}})^2$ where n_t is the number of time points, eliminating the possibility of a nonunique set of parameters. Our library is still being built up and tested, but from current tests the program successfully finds an "unknown" curve that is explicitly contained in the library and locates the correct region of the library given a curve derived from intermediate parameter values from any contained in the library. An example of this is given in Figure 9 in which an unknown curve is constructed from the average of length 50 and 100 chains with the parameters given in Table IV. The three best fits obtained are plotted in Figure 9, to compare the sensitivity of the $\alpha(t)$ curves. The parameters of these best fit curves are also given in Table IV. As can be seen from the data presented there, there is a trade-off between the value of ϕ and the number of traps.

However, the best choice (curve a) is exactly what one would expect, given the origin of the "unknown" curve.

One important consideration is the uniqueness of the different $\alpha(t)$ curves, which can be assessed as follows: The value of χ^2 between different members of the $\alpha(t)$ ensemble can be computed. If we assume that we can easily distinguish between curves with $\chi^2 \geq 1 \times 10^{-4}$, then for our present ensemble of 63 decays there are 13 pairs out of 1953 that have a χ^2 smaller than this limit and 138 with $\chi^2 \leq 5 \times 10^{-4}$. Thus the probability of a unique fit to an experimental $\alpha(t)$ curve is very high. The final assessment of the usefulness of this method awaits further testing and can only be determined through repeated trials. It is expected that a refinement "limit" will quickly be reached with this method, thus defining a range within which the actual parameters fall. Hopefully this range will be well-defined and small. While the time-dependent fractal dimensionality ($\alpha(t)$) was instituted to analyze EET on a polymer coil embedded in a cubic lattice, it may be useful to apply this method to DET or possibly even triplet energy transfer.

Summary

In this paper we have carried out explicit calculations of intrapolymer energy transfer from a donor to a trap with different values of the Förster trapping radius R_0 (eq 3) and with and without down-chain energy migration (the EET and DET cases, respectively). The polymer chain was simulated by a self-avoiding random walk on a cubic lattice with a segment-solvent interaction energy. Thus we can evaluate the relative sensitivity of the time-dependent donor fluorescence ($\langle S(t) \rangle$) to the extent of coil expansion for these two cases. Qualitatively we observe that DET gains sensitivity to the coil density as R_0 increases, while for the EET case there is considerable variation in $\langle S(t) \rangle$ for all values of R_0 (cf. Figures 1 and 4). However, it is clear that both cases lend themselves to conformational analysis.

One of the challenges of work of this type is the ability to analyze experimental data in terms of a physical model. We find the $\alpha(t)$ quantity defined in eq 12 and A and d_s from eq 16 to be useful in this regard. The values of these quantities vary in a systematic fashion with the physical parameters N , p , and ϕ . Thus the use of these quantities in the analysis of experimental data is likely (but not guaranteed) to yield a unique set of physical parameters in the context of a specific conformational model. We have employed two methods to invert experimental data: (1) derivation of an empirical relationship between a fitting function and physical parameters, followed by the solution of an algebraic equation; (2) a "pattern recognition" method in which the experimental $\alpha(t)$ is compared with a library of known functions. The former method has the advantage that anyone can use the derived empirical equation to analyze their experimental data while in the latter case the experimentalist must have the full library of $\alpha(t)$ curves. On the other hand, the derivation of a useful empirical equation requires a systematic variation of the experimentally derived quantities (e.g., A and d_s) with the physical parameters, which is not always the case, as we found with DET. The "pattern recognition" method is the most general and is easily accomplished with a computer library lookup program.

The methods employed herein permit calculation of $\langle S(t) \rangle$ for more realistic models of energy transport in disordered systems than has been possible in the past (polymers are just one example of this class of system). For the first time one can explicitly compare the effect of

coil expansion and donor-trap R_0 on the efficiency of photon harvesting by a trap species. In future theoretical work along these lines we anticipate examining the effect of a variation of energy-transfer rates between neighboring chromophores because of orientational and separational disorder or tacticity, the effect of polymer motions on the time scale of the excited state lifetime, and explicit consideration of the molecular structure of the polymer repeating unit.

Acknowledgment. This work was supported by the State of Texas Advanced Research Program (Grant No. 4652) and the National Science Foundation Polymers Program (Grant DMR-8614252) to S.E.W. R.A.F. acknowledges the financial support of the Robert A. Welch Foundation.

References and Notes

- (1) *Polymer Photophysics*; Phillips, D., Ed.; Chapman and Hall: London, 1985.
- (2) *Photophysics of Polymers*; Hoyle, C. E., Torkelson, J. M., Eds.; ACS Monograph Series 358; American Chemical Society: Washington, DC, 1987.
- (3) *Photophysical and Photochemical Tools in Polymer Science*; NATO Advanced Study Institute Series C; Winnik, M. A., Ed.; D. Reidel: Dordrecht, Holland, 1986; Vol. 182.
- (4) (a) Byers, J. D.; Friedrichs, M. S.; Friesner, R. A.; Webber, S. E. *Macromolecules* 1988, 21, 3402. (b) Byers, J. D.; Friedrichs, M. S.; Friesner, R. A.; Webber, S. E. in *Molecular Dynamics in Restricted Geometries*; Klafter, J., Drake, J. M., Eds.; John Wiley & Sons: New York, 1989; p 99.
- (5) van Rensburg, E. J. J.; Guillet, J. E.; Whittington, S. G. *Macromolecules* 1989, 22, 4212.
- (6) (a) Förster, T. *Ann. Phys. (Leipzig)* 1948, 2, 55. (b) Förster, T. *Z. Naturforsch.* 1949, 4A, 321. (c) See: Birks, J. *Photophysics of Aromatic Molecules*; Wiley-Interscience: New York, 1970.
- (7) Levitz, P.; Drake, J. M.; Klafter, J. *Chem. Phys. Lett.* 1988, 148, 557.
- (8) (a) Peterson, K. A.; Zimmt, M. B.; Linse, S.; Dominique, R. P.; Fayer, M. D. *Macromolecules* 1987, 20, 168. Peterson, K. A.; Fayer, M. D. In *Photophysics of Polymer Systems*; ACS Monograph Series 358; American Chemical Society: Washington, DC, 1987.
- (9) For a number of different examples, see: *Molecular Dynamics in Restricted Geometries*; Klafter, J., Drake, J. M., Eds.; John Wiley & Sons: New York, 1989.
- (10) Guillet, J. E. *Polymer Photophysics and Photochemistry*; Cambridge University Press: Cambridge, U.K., 1985; Section 9.8.
- (11) Nauts, A.; Wyatt, R. E. *Phys. Rev. Lett.* 1983, 51, 2238.
- (12) Friedrichs, M. S.; Friesner, R. A. *Chem. Phys. Lett.* 1987, 137, 285.
- (13) (a) Rosenbluth, M. N.; Rosenbluth, A. W. *J. Chem. Phys.* 1968, 49, 648. (b) McCrackin, F. L.; Mazur, J.; Guttman, C. M. *Macromolecules* 1973, 6, 859.
- (14) (a) Fitzgibbon, P. D.; Frank, C. W. *Macromolecules* 1982, 15, 733. (b) Gelles, R.; Frank, C. W. *Macromolecules* 1982, 15, 741. (c) Fredrickson, G. H.; Frank, C. W. *Macromolecules* 1983, 16, 572. (d) For a general review see: Frank, C. W.; Fredrickson, G. H.; Andersen, H. C. *Photophysical and Photochemical Tools in Polymer Science*; NATO Advanced Study Institute Series C; Winnik, M. A., Ed.; D. Reidel: Dordrecht, Holland, 1986; Vol. 182.
- (15) (a) Sienicki, K.; Mattice, W. L. *J. Chem. Phys.* 1989, 90, 6187. (b) Sienicki, K.; Mattice, W. L. *Macromolecules* 1989, 22, 2854. (c) Sienicki, K.; Mattice, W. L. *J. Lumin.* 1989, 43, 233.
- (16) Sienicki, K.; Winnik, M. A. *J. Chem. Phys.* 1987, 87, 2766.
- (17) Martinho, J. M. G.; Winnik, M. A. *J. Chem. Phys.* 1987, 91, 3640.
- (18) Klafter, J.; Blumen, A. *J. Chem. Phys.* 1984, 80, 874.
- (19) (a) Klafter, J.; Blumen, A.; Drake, J. M. In *Molecular Dynamics in Restricted Geometries*; Klafter, J., Drake, J. M., Eds.; John Wiley & Sons: New York, 1989; p 1. (b) Levitz, P.; Drake, J. M.; Klafter, J. In *Molecular Dynamics in Restricted Geometries*; Klafter, J., Drake, J. M., Eds.; John Wiley & Sons: New York, 1989; p 165.
- (20) Bai, F.; Chang, C.-H.; Webber, S. E. *Macromolecules* 1986, 19, 2484.
- (21) de Gennes, P.-G. *Scaling Concepts in Polymer Physics*; Cornell University Press: Ithaca, NY, 1979; Section I.2.

- (22) At very long times $\alpha(t)$ must approach unity. However, the survival probability may be so small by the time this limit is reached as to be irrelevant.
- (23) Preliminary data from D. Kiserow. These polymers are the same as reported in: *Macromolecules* **1989**, *22*, 2766.
- (24) Multiplication of an experimental decay curve by e^{+t/τ_D} tends to distort the curve in such a way as to increase the magnitude

of the residuals with time. It is probably more accurate to multiply the multiexponential fitting function by e^{+t/τ_D} in order to obtain a representation of $\langle S(t) \rangle$.

- (25) τ_D can be environmentally sensitive such that the use of a model compound or model polymers can lead to a misestimate of τ_D . τ_D can also be estimated from the smallest lifetime component of a multiexponential decay curve (i.e., $\tau_D \geq \tau_{\text{smallest}}$).